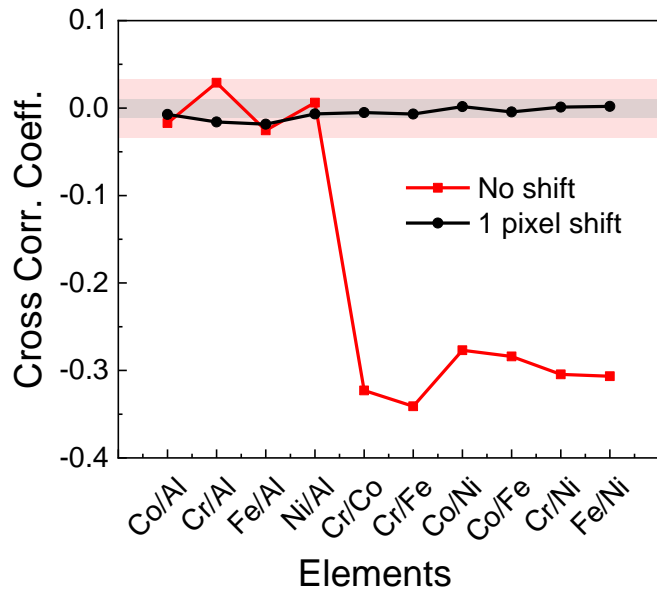
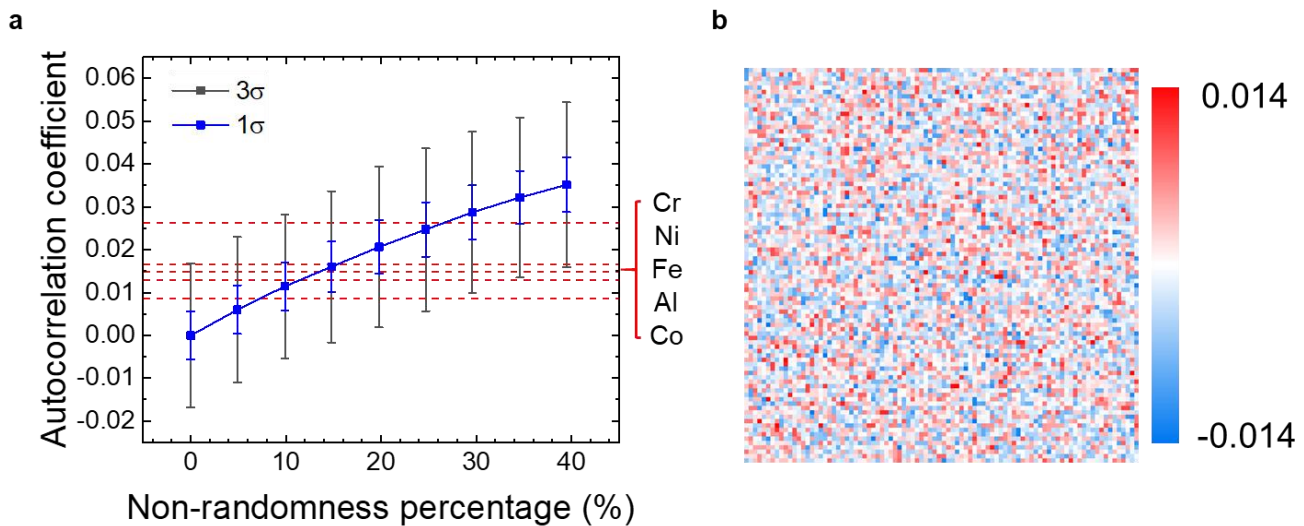


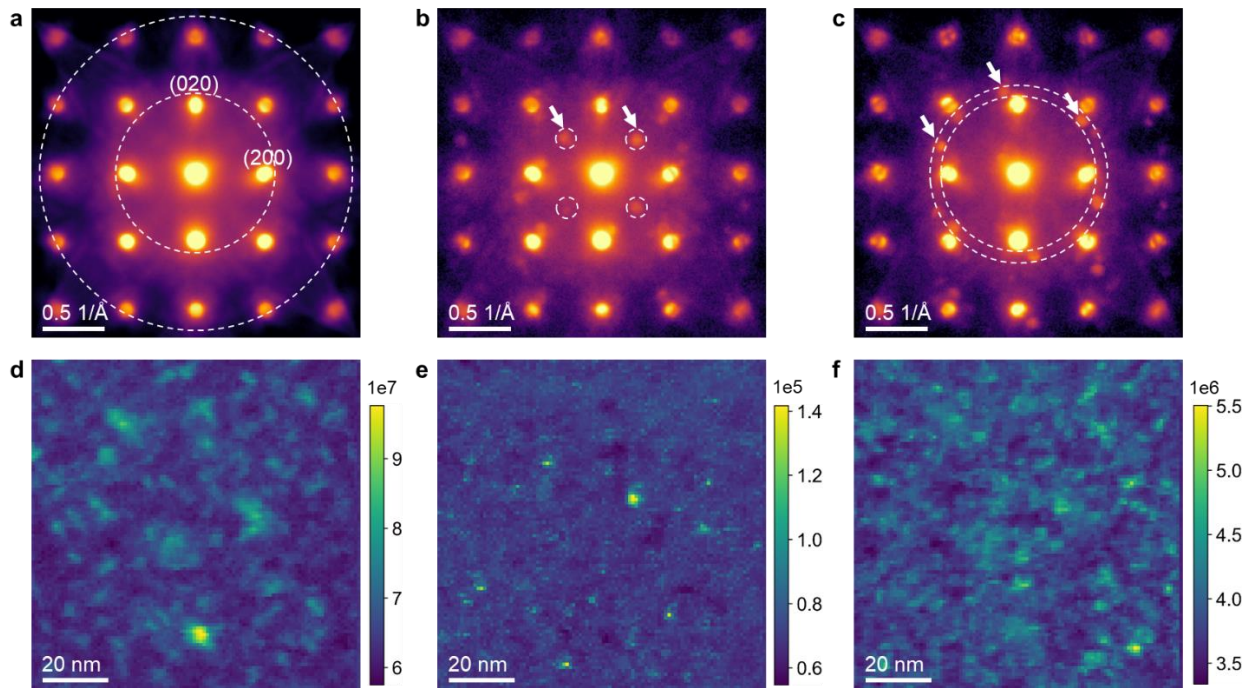
Extended Data Fig. 1 Chemical disorder in $\text{Al}_{0.1}\text{CrCoFeNi}$. (a) An averaged EDS spectrum from the STEM/EDS spectral dataset acquired over the $90 \times 90 \text{ nm}^2$ sample area with a step size of 1 nm. (b) An example of Cr-K peak fitting. (c-g) The peak-ratio maps extracted from the EDS dataset for each element in the HEA. The maps are displayed with the low and upper limits of ± 3 times of standard deviation about the average.



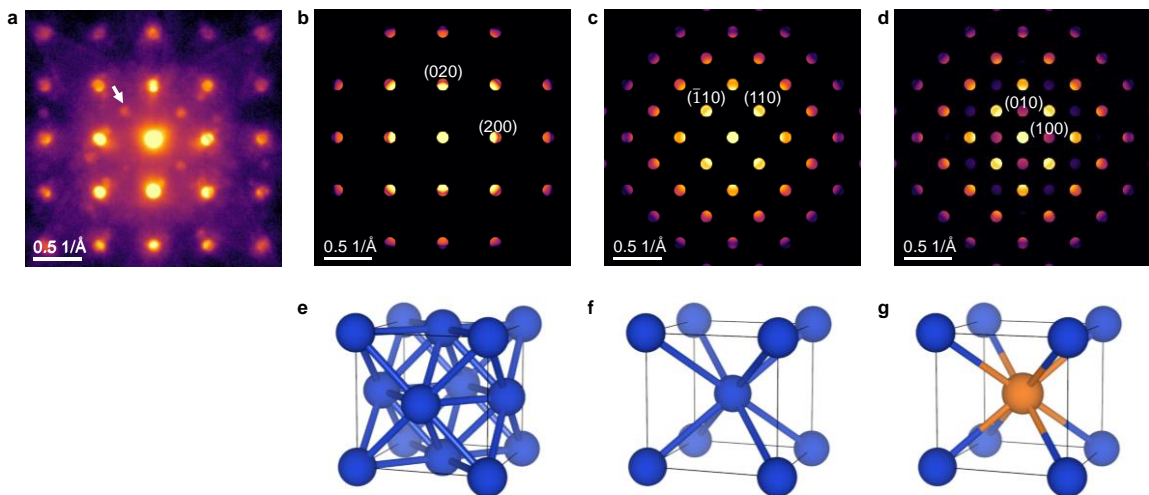
Extended Data Fig. 2 Cross-correlation of elemental combinations. For zero-pixel image shift, the red curve shows that Cr, Co, Fe and Ni have a negative correlation with each other, while the correlation of Al with other elements is under the limit of random model (red shadow region). At 1-pixel distance apart, the cross-correlation intensity falls within the limit of random model (gray shadow region) for all elements.



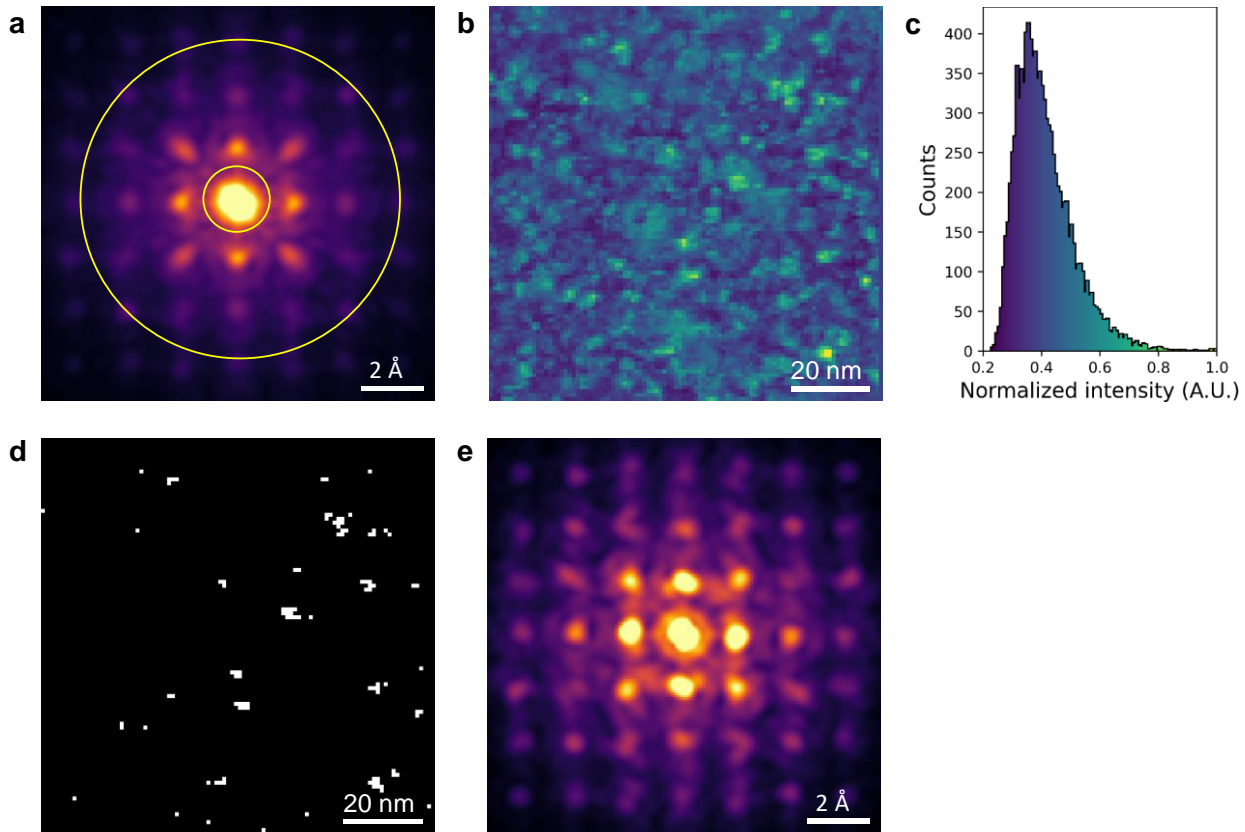
Extended Data Fig. 3 Effect of non-randomness on autocorrelation function (ACF). (a) The plot of ACF coefficient at $r = 1$ versus the percentage of non-randomness as obtained from simulations. Red dash lines indicate the ACF value of each element at 1 nm distance obtained from the STEM-EDS ratio maps. The bar in (a) marks $\pm\sigma$ and $\pm3\sigma$, estimated from the random model (Suppl. Note 2). (b) An example random image with 25% non-randomness sites.



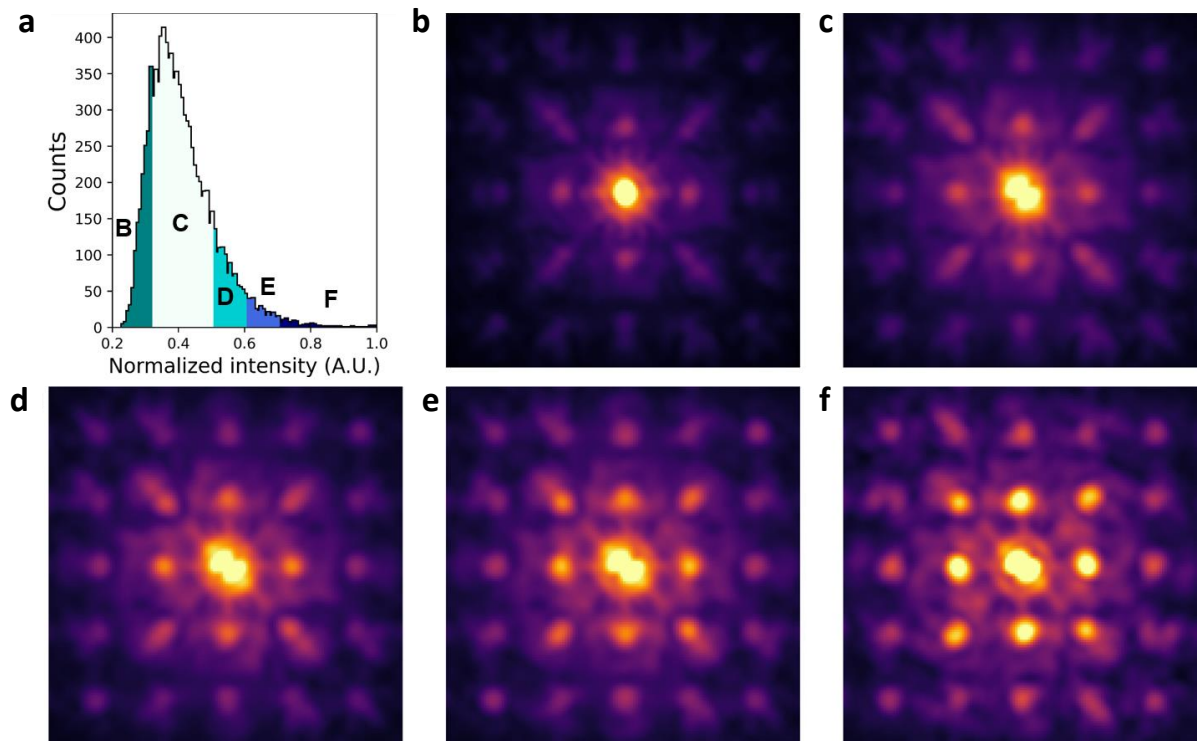
Extended Data Fig. 4 Electron nanodiffraction imaging of structural inhomogeneity. (a) Averaged diffraction pattern of an 100×100 SEND dataset, with step size of 1 nm. Selected individual diffraction patterns shown in logarithmic scale having (b) extra $\langle 110 \rangle$ reflections, and (c) extra reflections inside the dashed circles. (d) virtual ADF image constructed from the SEND dataset by integrating intensities between the dashed circles in (a), (e) Virtual DF image generated by integrating intensities inside the 4 dashed circles in (b). (f) Virtual ADF image integrated over the dashed circles in (c). The white arrows in (b & c) indicate extra reflections which do not belong to the FCC lattice.



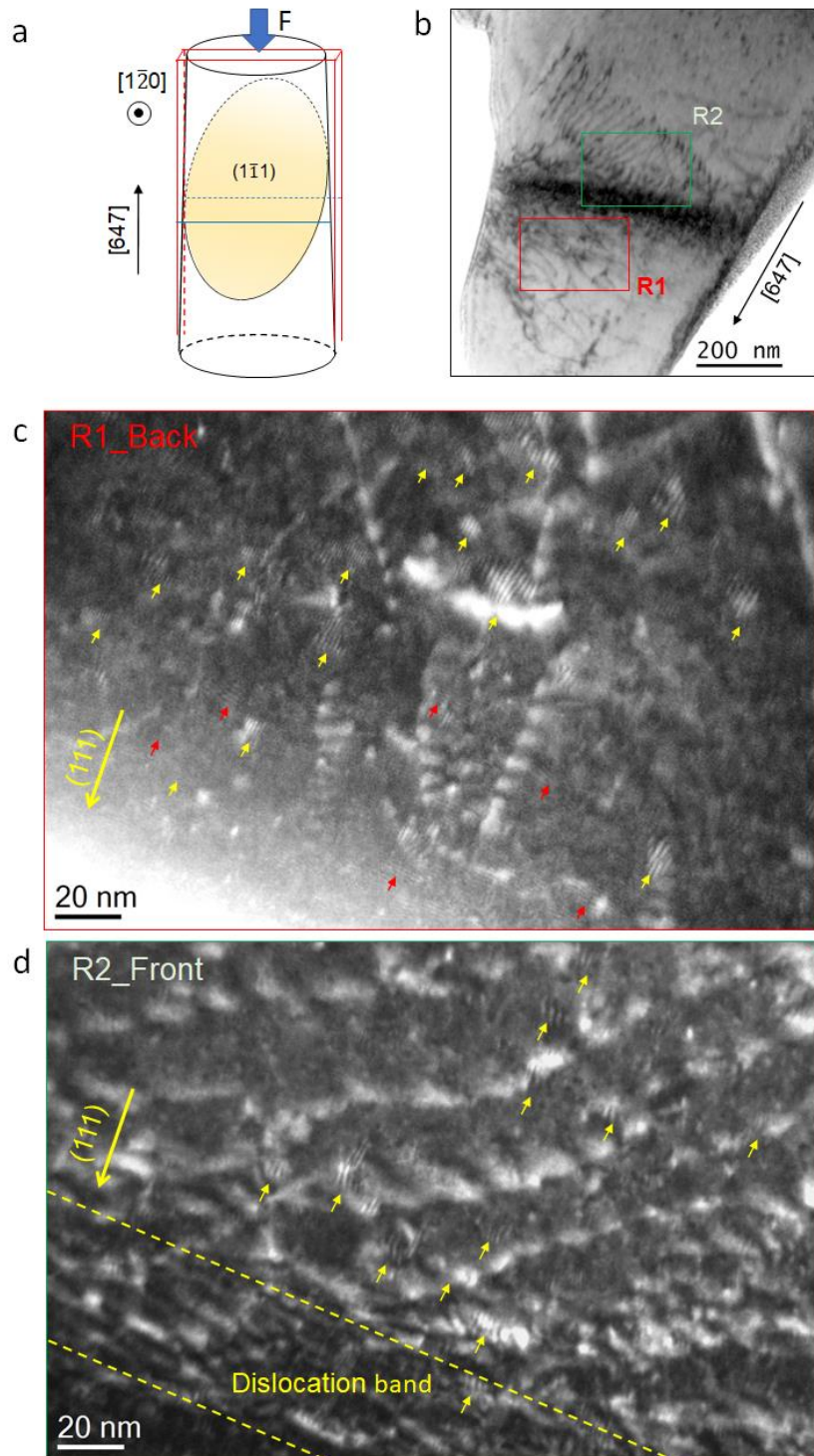
Extended Data Fig. 5 Electron diffraction phase analysis. (a) A recorded nanodiffraction pattern showing the extra $\langle 110 \rangle$ reflections. Corresponding simulated nanodiffraction patterns of (b) FCC structure, (c) BCC structure, and (d) B2 structure with Cr at the body center, with the Ball and stick structure models shown below in (e-g).



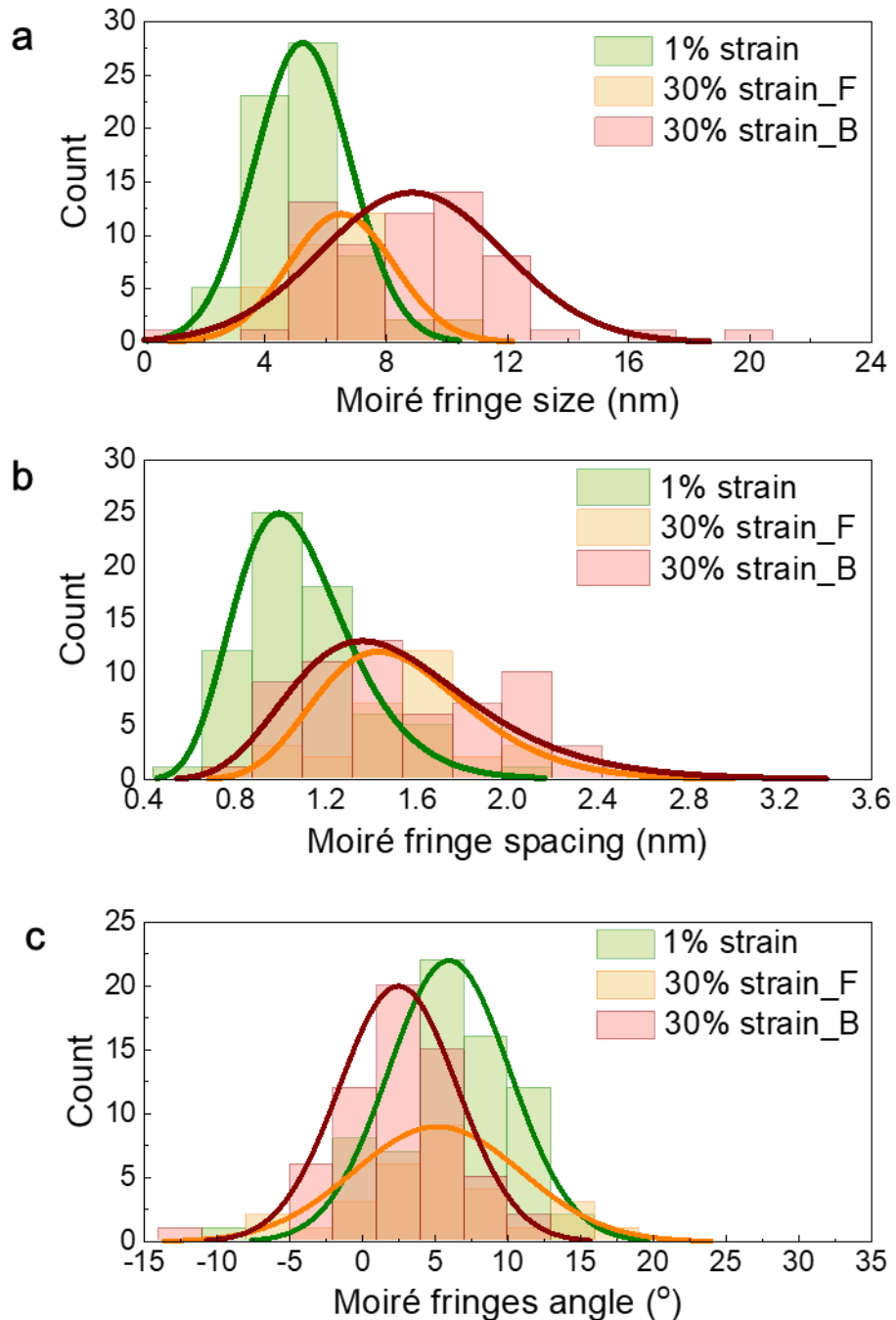
Extended Data Fig. 6 Histogram segmentation of the cepstral dataset. (a) Average of 10,000 difference cepstral patterns. (c) Histogram of the (b) Cepstral virtual ADF image reconstructed from the cepstral-transformed SEND dataset by integrating the correlation distances from $r=0.44\text{--}4.25\text{ \AA}$. (d) A masked image of (b) with values larger than 0.7 of the normalized intensity, and (e) Cepstral pattern obtained by averaging over the threshold regions in (d).



Extended Data Fig. 7 Difference Cepstral patterns based on histogram segmentation. (a) Histogram of virtual ADF image reconstructed from the cepstral-transformed SEND dataset by integrating the correlation distances from $r=0.44\text{--}4.25\text{ \AA}$. (b-f) Representative cepstral patterns for each segment indicated in the histogram in (a), obtained by averaging over the corresponding clustered regions.



Extended Data Fig. 8 Dislocation microstructure of a deformed HEA nanopillar. (a) Schematic illustration of nanopillar compression and cross-sectional geometry for post-mortem analysis. (b) A BF-TEM image showing the dislocation band and dislocation pileup in front of the dislocation band formed after compression to 30%. (c) and (d) DF-TEM images showing Moiré Fringes contrast regions with size ranging from ~6 to ~14 nm and dislocations in the deformed pillars in the front and back of the dislocation band. The red and yellow arrows mark two types of Moiré Fringes.



Extended Data Fig. 9 Distribution of Moiré fringes in the deformed nanopillars. At 30% strain, B and F stands for in the back and front of the dislocation band respectively, as shown in **Extended Data Fig. 8**. (a) the Moiré fringe size, (b) Moiré fringe spacing and (c) Angle between Moiré fringes and $g(111)$ direction